American Journal of Neural Networks and Applications
2024, Vol. 10, No. 2, pp. 27-35
https://doi.org/10.11648/j.ajnna.20241002.11

Research Article

Automated Lunar Surface Image Classification Using Deep Convolutional Neural Networks for Geological Feature Detection

J M Raisul Islam Shohag*

Civil Engineering Department, New Mexico State University, Las Cruces, USA

Abstract

Robotic rovers have vastly expanded our understanding of the lunar surface, providing detailed imagery crucial for scientific research and future exploration. However, manually classifying this imagery is time-consuming and prone to errors, necessitating automated solutions. Automated classification of lunar surface imagery is vital for efficient data analysis, site selection for future missions, and advancing lunar exploration. Developing accurate and efficient image classification systems tailored for lunar terrain is thus imperative. The objective of this study is to develop and assess an image classification system utilizing Deep Convolutional Neural Networks (DCNNs) specifically for lunar surface images. The aim is to achieve high accuracy and efficiency in identifying geological features such as craters and dunes, as observed by robotic rovers. A curated dataset of lunar surface images was partitioned into training, testing, and validation subsets. DCNNs models were trained on the training dataset and evaluated using testing and validation datasets. Hyperparameter tuning and optimization techniques were employed to enhance model performance. The classification system based on DCNNs showed promising outcomes. Model B and F achieved an accuracy of 91.1%, while Model A and D achieved 87.5%. Model C attained an accuracy of 89.3%, and Model E reached 83.9%. Visualizations of training and validation metrics revealed distinct performance patterns across models, highlighting the potential for further advancements in lunar exploration research.

Keywords

Lunar Surface Image, DCNNs, Hyperparameter Tuning, Optimization Techniques, Accuracy

1. Problem Description

The lunar surface, known for its diverse landscape and varied geological formations, offers both intriguing and challenging opportunities for exploration. Images captured by robotic rovers provide critical insights into the composition of moon and structure, acting as a gateway to its geological history [1].

Craters, as significant features, are more than mere depressions; they contain valuable information about the history of moon. Varatharajan I. et al. [2] emphasized that these craters are records of historical impacts and geological processes that have shaped the lunar landscape over time. Their widespread occurrence makes them essential for tasks such as age estimation through crater counting and understanding the geological evolution of the surface [3].

*Corresponding author: Ris.magura.ruet.ce130014@gmail.com (J M Raisul Islam Shohag)

Received: 27 September 2024; **Accepted:** 17 October 2024; **Published:** 31 October 2024

Wang S. et al. [4] highlighted the challenges associated with accurately recognizing craters. While human observation can lead to precise classifications, it is often time-consuming and inconsistent, with expert assessments differing by as much as 45% for the same lunar landform image [5]. This reliance on subjective interpretation underscores the urgent need for automated methods that can efficiently analyze large volumes of lunar imagery. Craters created by small impactors are key surface features on many bodies in the Solar System. On airless bodies like the Moon, the lack of weather-related erosion, tectonics, and volcanic activity has allowed for the accumulation of impact craters over time. As noted by Silburt A. et al. [6], crater densities provide a means to examine a body's geological history and assess the relative chronology of regions remotely. This emphasizes the importance of accurately identifying craters, as these records are vital for understanding Solar System formation theories. Additionally, lunar swirls, which are large albedo features found across the Moon, add complexity to lunar geology. Traditionally, these features have been mapped through visual inspection but identifying the boundaries between bright and dark regions can be subjective [7]. Recent studies utilizing machine learning techniques have improved the identification and mapping of swirls by providing measurable criteria, thus reducing bias and enhancing classification accuracy.

Within lunar surface imagery, various categories represent distinct geological phenomena. Craters are the most common feature, evidencing past impacts, while dark and bright dunes illustrate the interplay of light and shadow on the lunar surface. Other features, such as slope streaks, impact ejecta, Swiss cheese-like formations, and spider-like structures, further diversify the image catalog, each offering clues about the Moon's geological evolution. However, identifying and categorizing these images presents significant challenges. The rugged terrain, varying lighting conditions, and the presence of similar-looking features often confuse automated classification systems. Moreover, the vastness of the lunar surface and the sheer volume of image data necessitate efficient and accurate methods for analysis and classification. In this context, the main aim is to utilize artificial intelligence effectively in creating a reliable image classification system for lunar surface imagery.

To address these challenges, Wang S. et al. [4] noted the increasing reliance on artificial intelligence (AI) and machine learning techniques, particularly DCNNs. Their research indicates that DCNNs are effective in automating the detection and classification of lunar geological features, showing robustness against variations in image quality and noise—conditions frequently found in lunar imagery. Traditionally, crater detection has been performed manually through visual inspection. However, as Silburt A. et al. [6] pointed out, this method is impractical for the numerous kilometer- and sub-kilometer-sized craters on the Moon, resulting in human-generated databases that often lack comprehensive spatial or size data. To overcome this limitation, researchers have developed Crater Detection Algorithms (CDAs) that employ various techniques, including edge detection and neural networks, to automate classification. While these algorithms show promise, they face challenges in generalizing across unseen data due to the complex nature of craters.

As Downes L. M. et al. [8] observed, AI-driven approaches have revolutionized lunar exploration, enabling rapid and precise analysis of extensive image datasets. By training advanced neural networks on labeled datasets of diverse lunar surface images, researchers have created models capable of detecting subtle differences between geological features and accurately classifying images into their respective categories. The primary aim is to leverage artificial intelligence effectively to develop a reliable image classification system for lunar surface imagery.

2. Data Analysis

2.1. Raw Data

The original dataset comprises a large collection of 73,021 images capturing the lunar surface by robotic rovers. These images provide a comprehensive view of the terrain of Moon, highlighting various geological characteristics and formations. Each image is already categorized into specific groups based on the type of geological feature it depicts. These categories [9, 10] encompass craters, dark dunes, slope streaks, bright dunes, impact ejecta, swiss cheese-like formations, and spider-like structures, with each assigned a unique numerical label ranging from 0 to 7. The images exhibit a wide range of characteristics, including diverse lighting conditions, terrain textures, and geological formations. Some images capture the stark contrast between light and shadow, highlighting the topography of the lunar surface, while others reveal intricate details of geological features such as crater rims, dune patterns, and surface textures. Additionally, variations in resolution, perspective, and image quality add further complexity to the dataset, requiring careful preprocessing and analysis before classification.

2.2. Data Description & Selection

The dataset encompasses a vast collection of 73,021 images portraying the captivating lunar surface in exquisite detail. Each image, meticulously categorized into distinct geological features, offers a glimpse into the fascinating world of lunar geology. From the stark beauty of craters to the intricate patterns of dark dunes and slope streaks, these images encapsulate the diverse terrain and geological processes shaping the landscape of Moon. The selection process for these images was guided by a commitment to clarity, relevance, and representativeness. By prioritizing high-resolution images with optimal clarity, the essence of each geological category while minimizing ambiguity was captured. Furthermore, the selection criteria were designed to encompass a broad spectrum of geological formations, providing a

comprehensive representation of lunar surface features. This approach ensures that our dataset reflects the rich diversity of the geology of Moon, enabling robust analysis and classification across different geological categories.

Overall, the data serves as a valuable resource for training and validating artificial intelligence models for lunar surface image classification. By utilizing the DCNNs, the objective is to create a strong classification system capable of precisely categorizing 276 new images according to their geological content. This will enhance our comprehension of lunar geology and streamline future exploration missions.

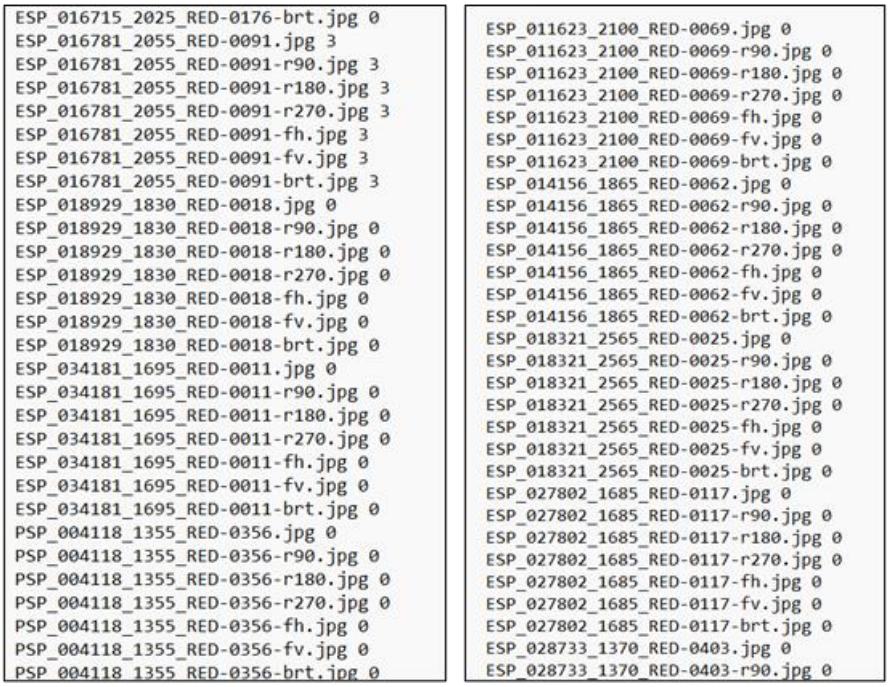

Figure 1. *Labelled lunar surface images taken by robotic rovers.*

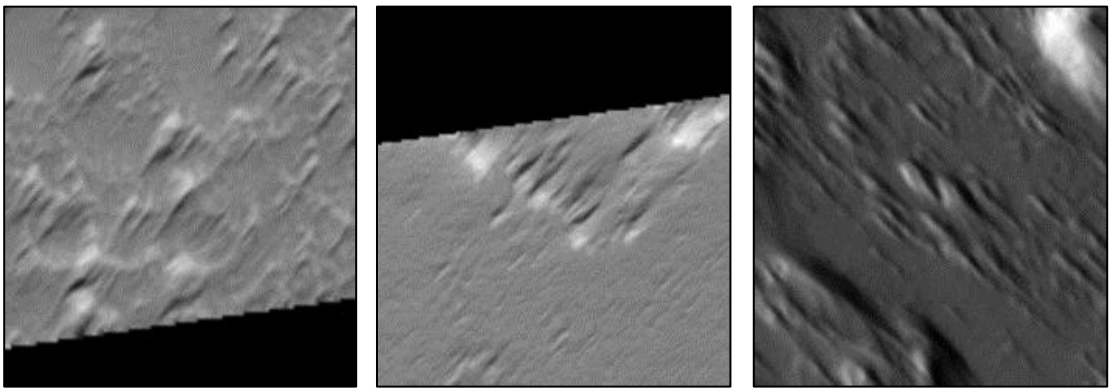

Figure 2. *Experimented images (276) for classification purposes.*

3. Description of Method

3.1. Convolutional Neural Networks

For extracting complex patterns and features from visual data DCNNs offer a powerful framework in the realm of image classification. With their structured design consisting of convolutional layers, pooling layers, and fully connected layers arranged in a hierarchy, DCNNs demonstrate proficiency in extracting significant representations from raw image inputs. The choice of DCNNs for the task of classifying images of the lunar surface is rooted in their innate ability to unravel the complexities inherent in lunar terrain. By automatically learning and extracting relevant features from the diverse array of geological formations captured in these images, DCNNs alleviate the need for manual feature engineering, thus streamlining the classification process. Crucially,

DCNNs exhibit translation invariance, enabling them to recognize patterns in images regardless of their spatial orientation or position. This property proves indispensable when classifying geological features on the lunar surface, where the arrangement and appearance of features can vary significantly from one image to another.

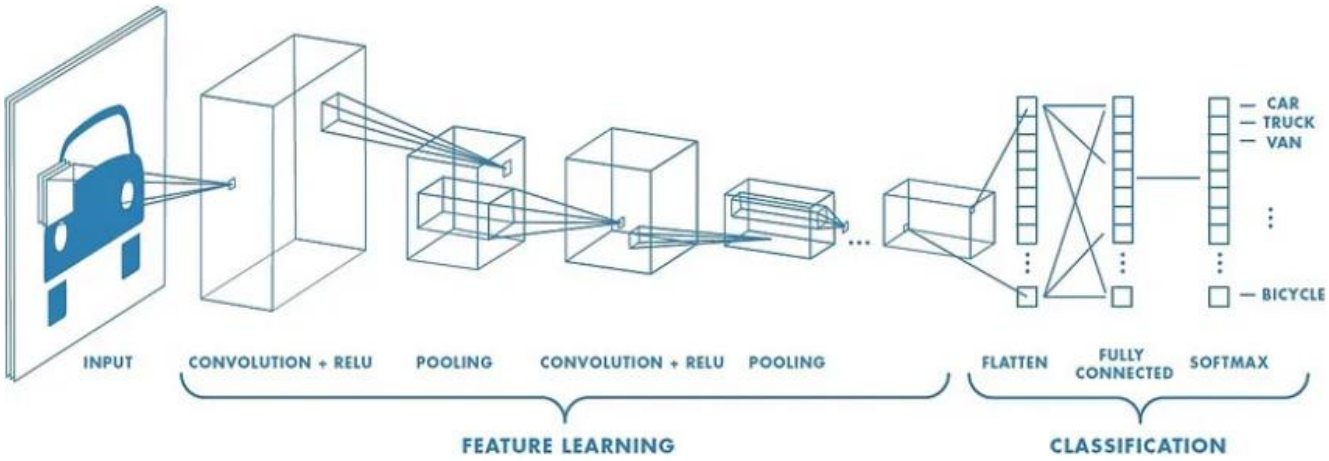

Figure 3. *The principle of DCNNs [11].*

A series of layers including convolutional, pooling, fully connected layers are the main structures of a typical DCNNs. The ReLU is the frequently utilized activation function in DCNNs. It introduces a level of complexity to the network, aiding in feature extraction.

In addition, in multi-class classification tasks, a softmax activation function is often applied to produce probability distributions across the output classes.

3.2. Hyperparameters

Key parameters significantly influence the performance and effectiveness of DCNNs when classifying lunar surface images. These parameters, such as kernel size, layer count, activation function, pooling size, dropout rate, and the choice of optimizer, play a crucial role in determining the efficacy of DCNNs. As Jafar A. and Myungho M. [12] explain, hyperparameter optimization involves selecting the optimal combination of hyperparameters to enhance model performance, focusing on both accuracy and computational efficiency. In the context of deep learning, this optimization can be understood as a process where inputs are processed by a function to yield outputs as numeric values, with the goal of finding parameters that maximize the function's output [13].

For example, the choice of kernel size influences the types of features the network can detect, ranging from large crater edges to fine surface textures. The number of layers within the network must achieve a balance between capturing complex patterns and avoiding overfitting, especially given the variability of lunar surface characteristics. Activation functions such as ReLU are instrumental in extracting nonlinear features, enabling the network to model the intricate relationships among various geological formations.

Pooling size is vital for down sampling feature maps while preserving essential characteristics, thereby ensuring efficient processing of extensive image datasets. Additionally, Jafar A. and Myungho M. [12] emphasize the importance of selecting appropriate hyperparameters in the training of deep neural networks [14]. The choice of hyperparameters can greatly influence model performance, as it helps maintain continuity between training steps, which can reduce oscillations. For instance, a high learning rate may lead to instability during training, while a low learning rate risks overlooking crucial patterns in the data. Therefore, identifying a suitable learning rate is essential for achieving optimal model performance without compromising computational efficiency.

Dropout regularization is effective in mitigating overfitting by randomly deactivating neurons during training, which enhances generalization, particularly in cases where labeled data is limited. Adjusting the learning rate is crucial for achieving stable convergence during training, allowing for efficient learning of features from lunar surface images. Furthermore, the selection of batch size plays a significant role in balancing computational efficiency with model stability, facilitating effective learning from the data. Ultimately, through careful tuning of these hyperparameters [15], a well-optimized DCNNs can successfully extract distinguishing features from lunar surface images, leading to precise classification of geological formations and deepening our understanding of lunar geology.

4. Results

Convolutional Neural Networks

In this investigation, the DCNNs were effectively deployed to classify 276 lunar surface images. The structure of the network is determined by hyperparameters such as kernel size,

network depth, and network width. Specifically, the DCNNs comprise three convolutional layers having a 3 x 3 size and utilizing of ReLu function, where the first layer possesses 32 filters and subsequent layers each contain 256 filters. To down sample the feature maps, max pooling (2, 2) is also used properly. A dense layer with 512 neurons is successfully applied to prevent overfitting. Subsequently, the output layer utilizes an activation function, softmax, to generate probabilities across classes for multi-class classification tasks. The entire network is optimized using the SGD optimizer, although specific values for learning rate, momentum, and weight decay are not explicitly provided. Table 1 outlines the hyperparameters associated with network structures. Before constructing the model, the dataset was divided into three subsets: training (60%), testing (20%), and validation (20%). The training set comprises 165 images, while the testing and validation sets consist of 56 and 55 images, respectively. All images have dimensions of 128 x 128 pixels with three color channels.

Table 1. *Hyperparameters related to Network Structures.*

Model (A, B, C, D, E, F)		
Hyperparameters related to Network Structures	**Value**	**Remarks**
Kernel size	(3,3)	First Conv2D layer: 32 filters, Second and Third Conv2D layer: 256 layers
Network depth	3	
Network width	(32, 256, 256)	

We utilized various parameters in training models A through F, encompassing a dropout rate of 0.2, momentum set at 0.9, weight decay of 0.01, and classification into 4 output classes. Additionally, incorporating leaky ReLU activation with a factor of 0.01, we employed mini-batch sizes of 32 and 64. Each model underwent a different number of epochs—models A and D were trained for 50 epochs, models B and E for 100 epochs, and models C and F for 150 epochs—with corresponding learning rates of 0.1, 0.01, and 0.001, respectively. During testing, model A exhibited a test loss of 47% and achieved an accuracy of 87.5%. Model B displayed a reduced loss of 22.5% and achieved an accuracy of 91.1%. Model C demonstrated a loss of 39% and an accuracy of 89.3%. Model D, E, and F showed losses of 46.3%, 40%, and 42% respectively, with corresponding accuracies of 87.5%, 84%, and 91.1%. These findings highlight the varied performance of the models under different training configurations. Detailed parameters are provided in.

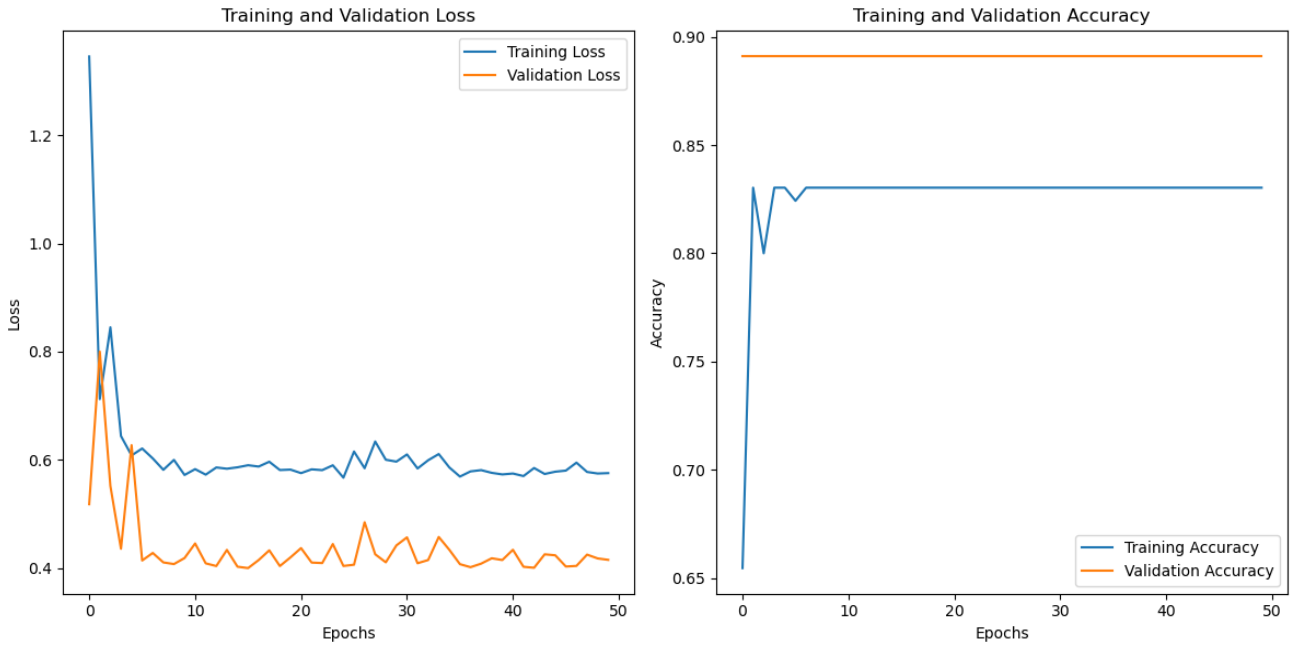

Figure 4. *Performance metrics for Model A.*

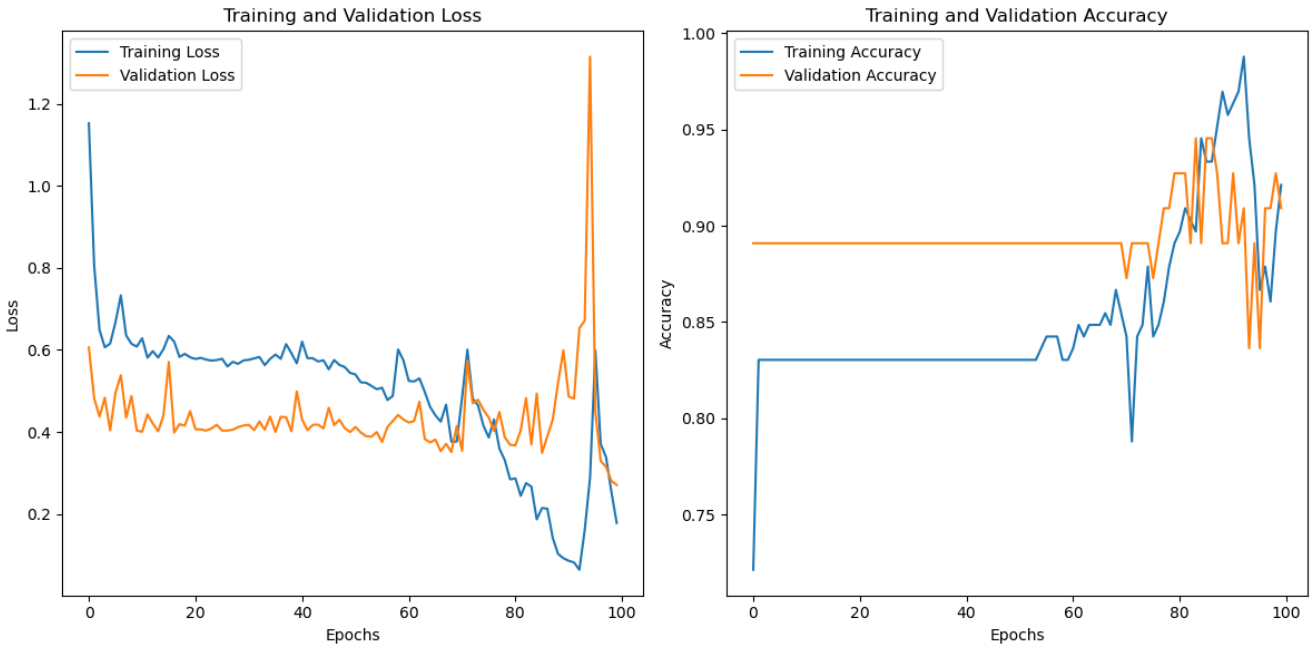

Figure 5. *Performance metrics for Model B.*

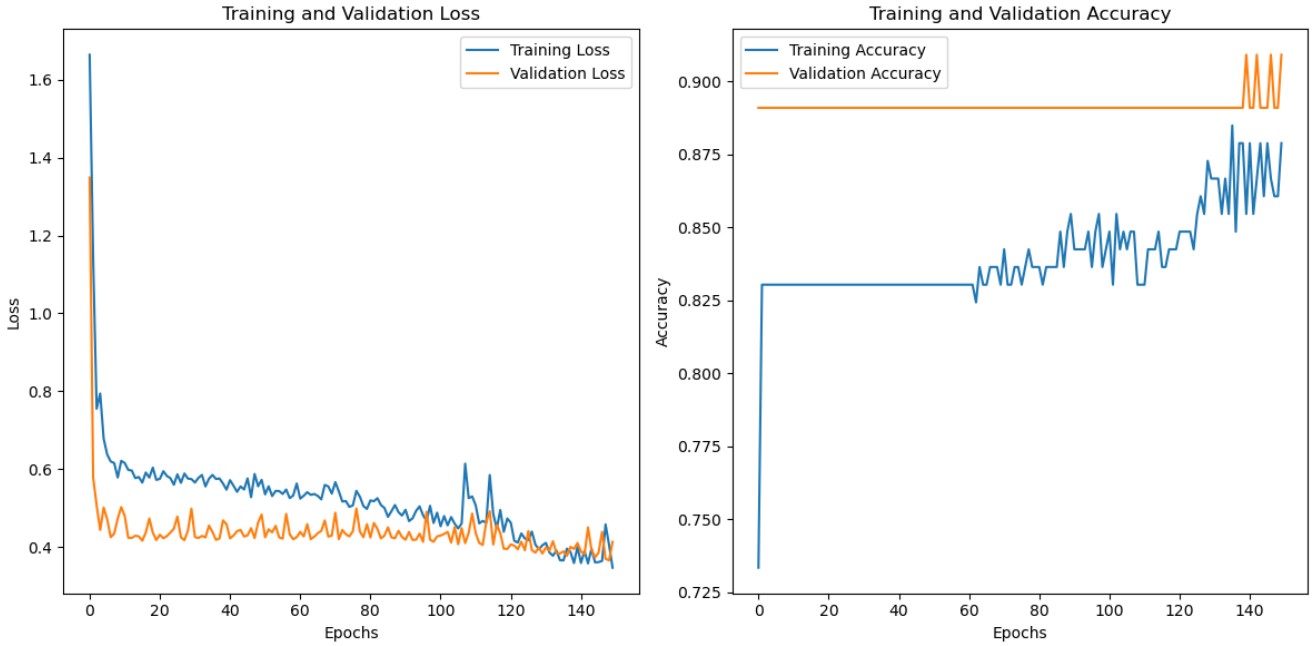

Figure 6. *Performance metrics for Model C.*

Table 2. *Parameters relevant to training the model.*

Model	Number of epochs	Learning rate	Batch size
A	50	0.1	32
B	100	0.01	32
C	150	0.001	32
D	50	0.1	64
E	100	0.01	64
F	150	0.001	64

In Model A, training and validation losses closely align, with validation consistently lower, while accuracy remains stable at 85% and 89%, respectively. Conversely, in Model B, initial validation loss is lower than training, but trends reverse

after 70 epochs. Model C exhibits similar behavior with a shift occurring after 130 epochs. Throughout, validation accuracy consistently outperforms training.

In the combined analysis of models D, E, and F, distinct patterns emerge. Initially, model D shows fluctuations where validation loss surpasses training loss, but after 5 epochs, validation loss decreases while training loss increases. Validation accuracy consistently exceeds training accuracy over 50 epochs, despite some fluctuations. Conversely, in model E, validation loss starts lower than training loss, but after 80 epochs, this trend reverses with maintained fluctuations. Validation accuracy consistently surpasses training accuracy, but towards the end of 100 epochs, this relationship reverses again. Throughout 150 epochs, model F consistently exhibits lower validation loss than training loss. Validation accuracy stabilizes at 90% without fluctuations, while training accuracy mostly maintains around 83% with minor fluctuations.

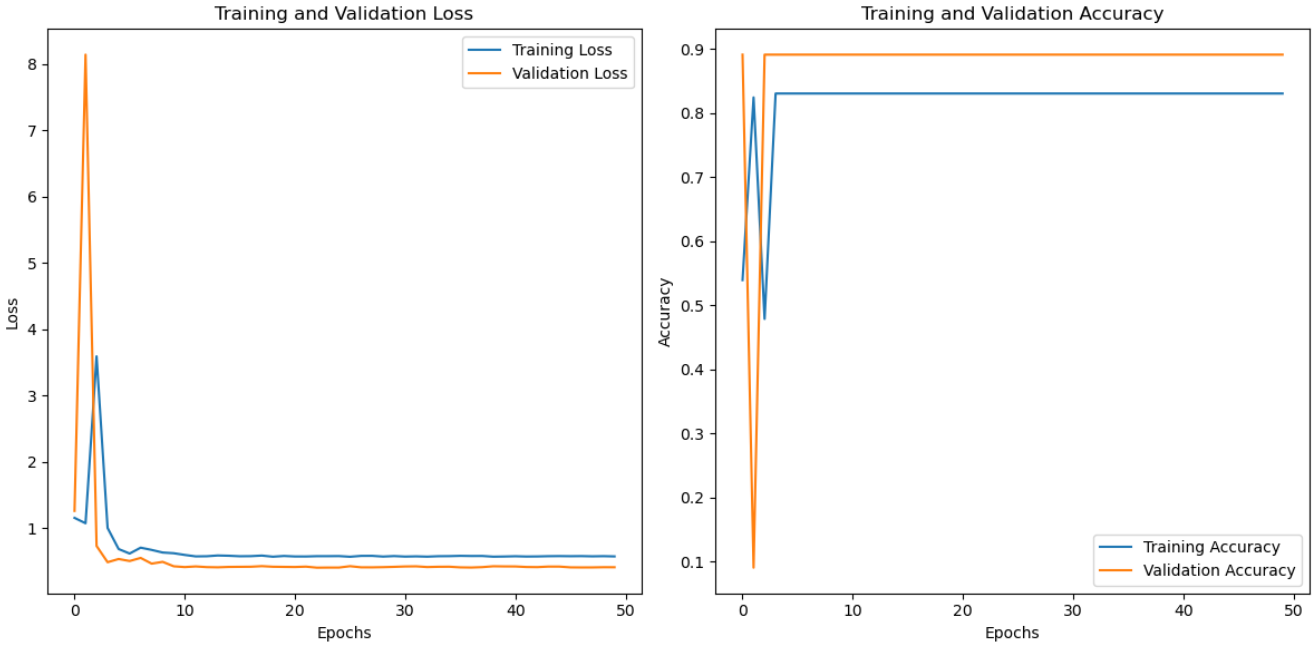

Figure 7. *Performance metrics for Model D.*

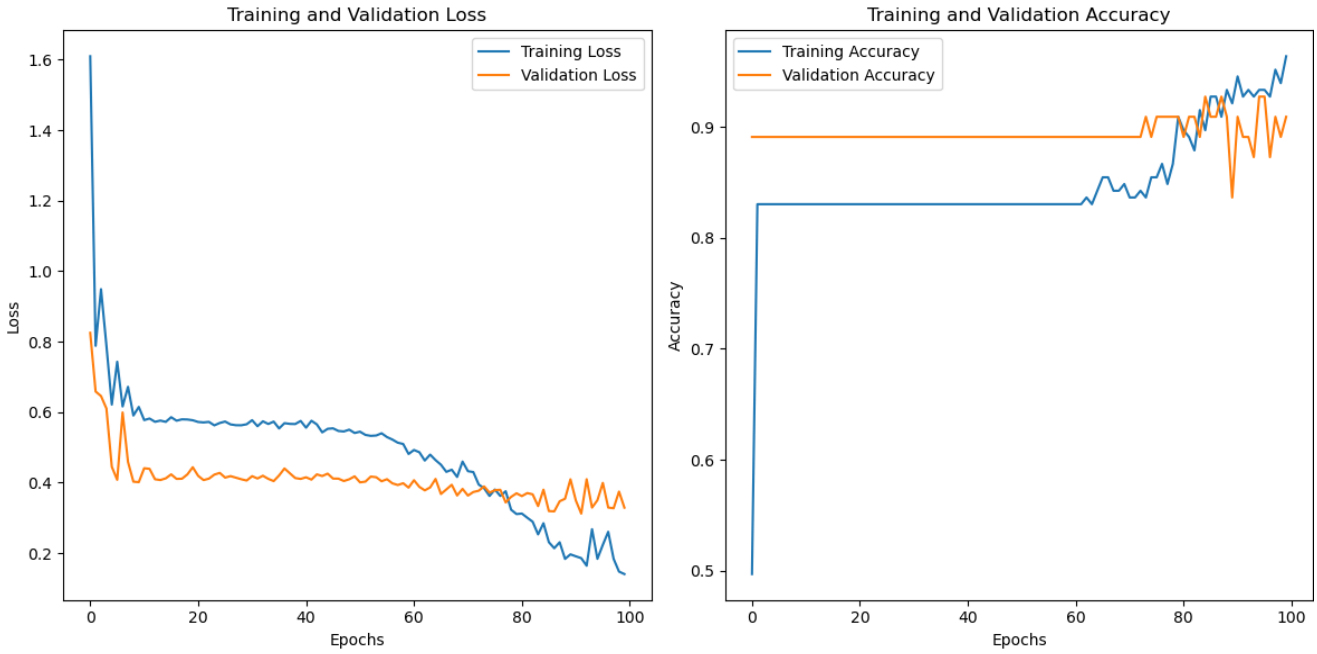

Figure 8. *Performance metrics for Model E.*

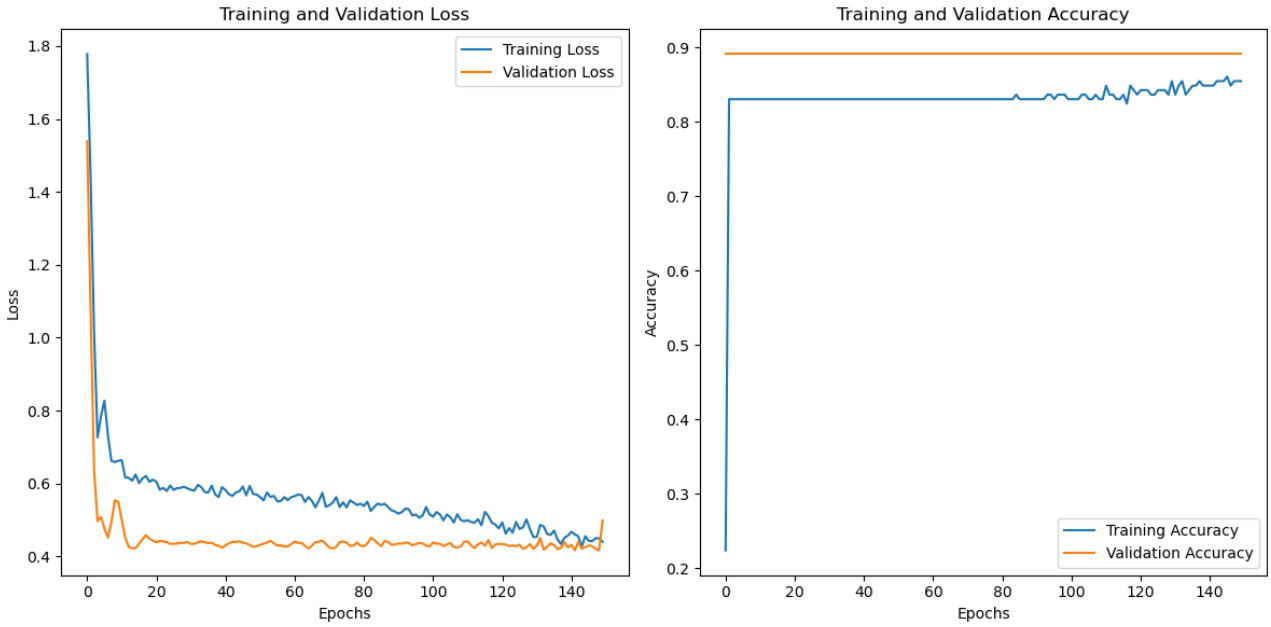

Figure 9. *Performance metrics for Model F.*

Abbreviations

DCNNs	Deep Convolutional Neural Networks
CDAs	Crater Detection Algorithms
AI	Artificial Intelligence

Author Contributions

J M Raisul Islam Shohag is the sole author. The author read and approved the final manuscript.

Ethical Approval

This study did not involve human participants or animal subjects; therefore, no ethical approval was required. The research was focused on the classification of lunar surface images using artificial intelligence. All data used in this study were publicly available and obtained from open-source repositories, ensuring compliance with relevant data usage and privacy guidelines.

Conflicts of Interest

The author declares no conflicts of interest.

References

[1] L. M. Downes, T. J. Steiner, and J. P. How, "Neural network approach to crater detection for lunar terrain relative navigation," *J. Aerosp. Inf. Syst.*, vol. 18, no. 7, pp. 391–403, 2021.

[2] I. Varatharajan *et al.*, "Artificial intelligence for the advancement of lunar and planetary science and exploration," *Bull. Am. Astron. Soc.*, vol. 53, no. 4, p. 222, 2021.

[3] V. J. Bray, G. S. Collins, J. V. Morgan, and P. M. Schenk, "The effect of target properties on crater morphology: Comparison of central peak craters on the Moon and Ganymede," *Meteorit. Planet. Sci.*, vol. 43, no. 12, pp. 1979–1992, Dec. 2008, https://doi.org/10.1111/j.1945-5100.2008.tb00656.x

[4] S. Wang, Z. Fan, Z. Li, H. Zhang, and C. Wei, "An Effective Lunar Crater Recognition Algorithm Based on Convolutional Neural Network," *Remote Sens.*, vol. 12, no. 17, p. 2694, Aug. 2020, https://doi.org/10.3390/rs12172694

[5] S. J. Robbins *et al.*, "The variability of crater identification among expert and community crater analysts," *Icarus*, vol. 234, pp. 109–131, May 2014, https://doi.org/10.1016/j.icarus.2014.02.022

[6] A. Silburt *et al.*, "Lunar crater identification via deep learning," *Icarus*, vol. 317, pp. 27–38, Jan. 2019, https://doi.org/10.1016/j.icarus.2018.06.022

[7] F. C. Chuang, M. D. Richardson, J. R. Weirich, A. A. Sickafoose, and D. L. Domingue, "Mapping Lunar Swirls with Machine Learning: The Application of Unsupervised and Supervised Image Classification Algorithms in Reiner Gamma and Mare Ingenii," *Planet. Sci. J.*, vol. 3, no. 10, p. 231, Oct. 2022, https://doi.org/10.3847/PSJ/ac8f43

[8] L. Downes, T. J. Steiner, and J. P. How, "Deep Learning Crater Detection for Lunar Terrain Relative Navigation," in *AIAA Scitech 2020 Forum*, Orlando, FL: American Institute of Aeronautics and Astronautics, Jan. 2020. https://doi.org/10.2514/6.2020-1838

[9] S. Hashimoto and K. Mori, "Lunar crater detection based on grid partition using deep learning," presented at the 2019 IEEE 13th International Symposium on Applied Computational Intelligence and Informatics (SACI), IEEE, 2019, pp. 75–80.

[10] H. S. Shin and S. C. Hong, "A deep-learning based automatic detection of craters on lunar surface for lunar construction," *KSCE J. Civ. Environ. Eng. Res.*, vol. 38, no. 6, pp. 859–865, 2018.

[11] "Deep Convolutional Neural Networks (DCNNs) explained in layman's terms." [Online]. Available: https://medium.com/aiguys/deep-convolutional-neural-networks-dcnns-explained-in-layman-terms-b990b2818061

[12] A. Jafar and L. Myungho, "Hyperparameter Optimization for Deep Residual Learning in Image Classification," in *2020 IEEE International Conference on Autonomic Computing and Self-Organizing Systems Companion (ACSOS-C)*, Washington, DC, USA: IEEE, Aug. 2020, pp. 24–29. https://doi.org/10.1109/ACSOS-C51401.2020.00024

[13] L. Getoor and International Machine Learning Society, Eds., *Proceedings of the Twenty-Eighth International Conference on Machine Learning: Bellevue, Washington, USA, June 28 - July 2, 2011*. Madison, 2011.

[14] X. Zhang, X. Chen, L. Yao, C. Ge, and M. Dong, "Deep Neural Network Hyperparameter Optimization with Orthogonal Array Tuning," in *Neural Information Processing*, vol. 1142, T. Gedeon, K. W. Wong, and M. Lee, Eds., in Communications in Computer and Information Science, vol. 1142. Cham: Springer International Publishing, 2019, pp. 287–295. https://doi.org/10.1007/978-3-030-36808-1_31

[15] A. A. Chowdhury, A. Das, K. K. S. Hoque, and D. Karmaker, "A comparative study of hyperparameter optimization techniques for deep learning," presented at the Proceedings of International Joint Conference on Advances in Computational Intelligence: IJCACI 2021, Springer, 2022, pp. 509–521.